

REAL TIME DIGITAL SIGNAL ANALYSIS AND MEASUREMENT

M. BAKKALI, C. MASCAREÑAS-PEREZ-IÑIGO

Abstract—We present in this paper a powerful low-cost method for real-time digital signal analysis and measurement based Discrete Fourier Transform. This measurement system needs understanding the mathematical background and the computational implementation, using the adequate cables, connectors, as well as having knowledge and experience for interpreting the results obtained. This paper tries to understand the fundamental concepts in DFT-based measurements, providing a better comprehension of the measured parameters, procedures, and interpreting the resulting data.

We attempt to make this paper summarized as much as possible; at the same time, to treat the most important aspects showing the different stages implemented into the system developed.

Keywords— Signal Analysis, Signal Measurement, DFT, FFT, Leakage, Window, Averaging.

I. Introduction

The system measurement that we present in this paper (figure 1) is a computer-based measurement that takes a continuous signal at its input, and samples it into a sequence of a discrete data $x(n)$. This periodic sampling is achieved using the PC sound card. The discrete-time signal is then converted from the time domain to the frequency domain through the calculation of the Discrete Fourier Transform DFT [1-3] to estimate the spectrum [4]. We use the Fast Fourier Transform FFT algorithm [5-8] for the DFT implementation. Windowing is a technique used to reduce the leakage effect. With the presence of the background noise, it is difficult to detect the signal of interest; for this reason, we use some averaging techniques in order to reduce the background noise and extract a signal from the noise. We close with a summary of the measurement parameters showing its effect on the analysis procedure. Here, we describe the different stages of the system developed.

We use the term main lobe to refer to the energy of the principal frequency component of the input signal.

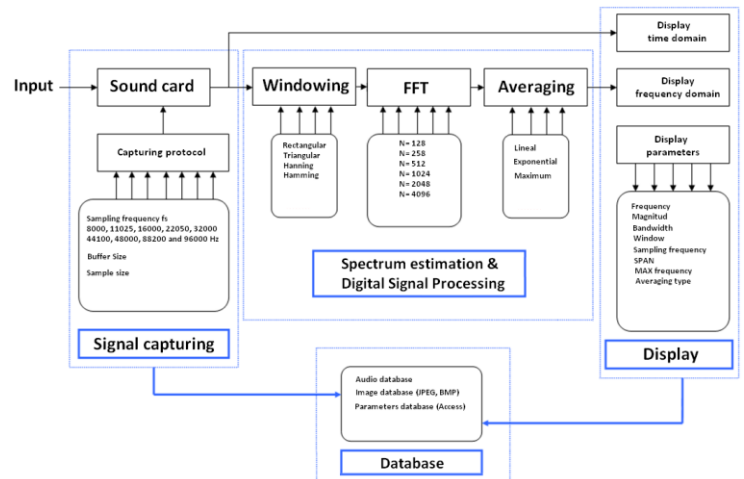


Figure 1. System measurement Bloc diagram

II. Sampling

In the input we have the signal to be analyzed which is an analog signal. The first stage is the periodic sampling which takes in its input, the analog signal, and gives us in its output, a sequence of discrete data values.

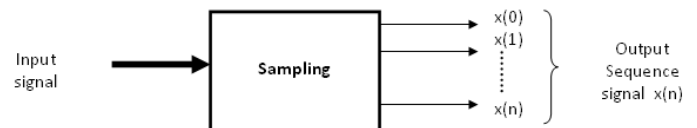


Figure 2. Sampling stage

The sequence of samples is an approximation that represents the original input signal in the digital domain, and must respect the condition imposed by the Nyquist's theorem: the sampling rate must be greater than twice the highest frequency component of the signal to be sampled. For example if we want to analyze an input signal containing various frequency components whose maximum value is 100 kHz, then the sampling frequency f_s must be as minimum 200 kHz. If this condition is not respected a phenomena known as aliasing occurs [1,2]. The frequency components that are above the Nyquist frequency are undersampled, and appear as lower frequency components. For this reason, in the practice, an analogue filter is used at the end of the sampling stage, in order to attenuate all unwanted frequency components above our analysis range. This filter is named anti-aliasing filter.

M. Bakkali is with Departamento Control y Comunicaciones, División Air Thermodynamics, CIAT, Cordoba, Spain.
medcasem@hotmail.com – mbakkali@grupociat.es

C. Mascareñas-Perez-Iñigo is with Departamento de CC y TT de Navegación y Teoría de la Señal y Comunicación, Cadix University, Cadix, Spain.
carlos.mascarenas@uca.es

III. Signal Capturing

Several implementations can be used to capture the waveform using a data acquisition device. Nowadays, advanced techniques known as “simultaneous multi-buffer acquisition and readout (SAR) mode [9]” is used to improve the precision of the capturing method with no information lose, specially used in the case of measuring pulse that can appear in a very short time. In our application we use the double buffering technique. It consists of using two buffers in order to achieve the processes of continuous capturing without loss of data. While one buffer is capturing data, the other is making the processing task. The figure 3 describes this process.

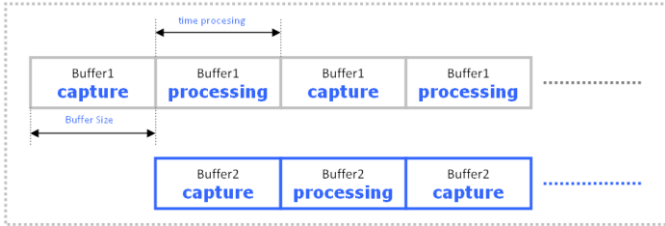


Figure3. Capturing process protocol used

Time processing stage will include DFT calculating (FFT algorithm), windowing, plotting, and averaging. This time must be inferior to the time that takes the buffer to capture the samples. If this condition is not respected, we lose information's when the device is waiting for a new buffer, and if some signal appears at that moment our analysis method will not be able to detect this signal. To overcome this problem, a possible solution is to use more buffers if the system implementation allows it, or reduce some operations from the processing stage. The size of the buffer must be an integral multiple of the every sample size (for example if we work with 16 bits each sample size, we can take a buffer as $N_DFT * 2 * 16$ bits).

IV. Discrete Fourier Transform

After the stage of the sampling, the next step is to convert the signal from the time domain to the frequency domain. This is achieved by the Discrete Fourier Transform DFT which is a mathematical calculation used to detect the frequency components and the energy presented at this input signal component. A different method can be used to estimate the spectrum [4], and the most famous algorithm for the DFT calculation is the Fast Fourier Transform known as FFT.

we take a N_DFT sample to achieve the DFT calculated by applying the FFT algorithm. The input is a sequence $x(n)$

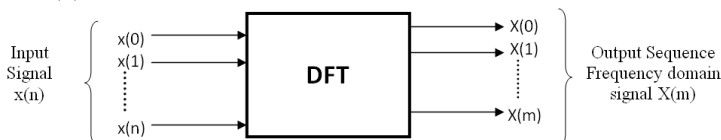


Figure 4. DFT stage calculation

As we are taking a finite number of points every time, this situation is similar to multiplying the sampled input sequence by a rectangular window of value 1 as shown in the figure 5.

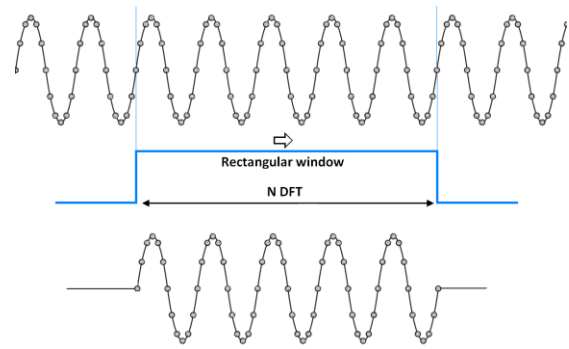


Figure 5. representation of the rectangular windowing effect
The figure 5 is only a representation that seems to be as a perfect situation, because the size of the DFT was chosen to fit exactly an integer number of cycles (in this example 5 cycles). This situation is difficult to occur in the real time signal acquisition. (For example if we want to measure a 1.6 kHz sine-wave taking 512 sample at a rate of 8 kHz per second, we may have to treat 102.4 cycles every time loop). The figure 6 represents an approximation of what we are taking in the real situation.

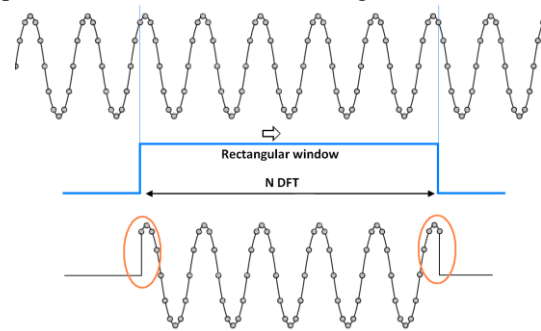


Figure 6. representation of the rectangular windowing leakage effect
In addition to the case of non-integer cycle mentioned above, we have discontinuity at the beginning and at the end of the rectangular window. These two factors may cause the Leakage [1,2].

V. Windowing

In order to reduce the leakage effect we use the windowing technique. The input sequence $x(n)$ is multiplied by a function window $w(n)$ before the DFT is performed.

$$X_w(m) = \sum_{n=0}^{N-1} w(n).x(n)e^{-j2\pi mn/N}$$

Rectangular window

$$w(n) = 1 \text{ for } n = 0, 1, 2, \dots, N-1$$

Triangular window

$$w = \begin{cases} \frac{n}{N/2} & \text{for } n = 0, 1, 2, \dots, N/2 \\ 2 - \frac{n}{N/2} & \text{for } n = N/2 + 1, N/2 + 2, \dots, N-1 \end{cases}$$

Hanning window

$$w(n) = 0.5 - 0.5 \cos\left(\frac{2\pi n}{N}\right) \text{ for } n = 0, 1, 2, \dots, N-1$$

Hamming window

$$w(n) = 0.54 - 0.46 \cos\left(\frac{2\pi n}{N}\right) \text{ for } n = 0, 1, 2, \dots, N-1$$

Blackman window

$$w(n) = 0.42 - 0.5 \cos\left(\frac{2\pi n}{N}\right) + 0.08 \cos\left(\frac{4\pi n}{N}\right)$$

for $n = 0, 1, 2, \dots, N-1$

Blackman-Harris window

$$w(n) = 0.36 - 0.49 \cos\left(\frac{2\pi n}{N}\right) + 0.14 \cos\left(\frac{4\pi n}{N}\right) - 0.01 \cos\left(\frac{6\pi n}{N}\right)$$

for $n = 0, 1, 2, \dots, N-1$

We put an example measuring the leakage effect by using a 13 kHz sine wave signal modulated with 9MHz AM. The figure 7a shows the signal obtained in the frequency domain with no window applied (rectangular window), while the figure 7b shows how the window, in this case a Hanning window, reduce the effect of leakage.

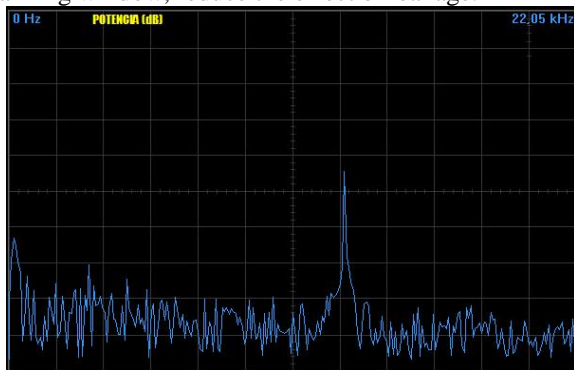
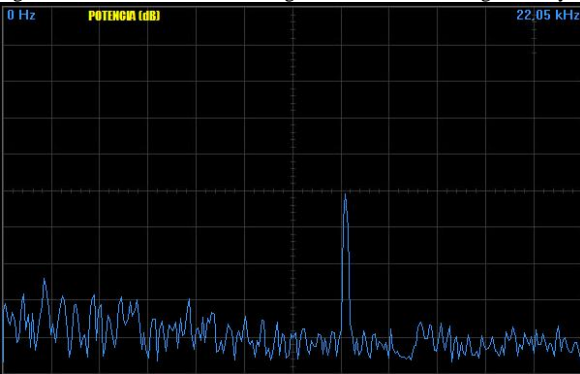


Figure 7a. illustration of the leakage effect in real time signal analysis



Applying a Window reduce the leakage effect, but at the same time reduce the magnitude of the output, for this reason, it is necessary to multiply the output magnitude DFT value by a *scaling factor* [10]. Table 1 shows the different scaling factor for the different window used in our measurement system.

TABLE 1: DIFFERENT SCALING FACTOR FOR THE DIFFERENT WINDOW

Window	Scaling Factor
Rectangular	1
Hamming	0.54
Blackman	0.42
Blackman-Harris	0.42
Hanning	0.50

Notice that the main lobe in the case of rectangular window is narrower; this is due to the effect of the window on increasing the effective bandwidth by a factor known as the *equivalent noise power bandwidth of the window* [10].

VI. The Parameters Used For The Analysis

Let's see the most important parameter to manipulate when we are dealing with the signal analysis. It is important to keep in mind that we take N sample points to produce N/2 useful frequency point (DFT symmetry propriety), the highest frequency of the analysis depends on the sampling rate $f_{max} = f/2$, The anti-aliasing filter will cut off all frequency components higher than a specific value which depends on the filter frequency (f_c), The lowest frequency will depend to the minimal time to perform one DFT cycle.

The parameters that we can modify in our system measurement are:

- The frequency of the data sampling ($f's$)
- Number of points used, or the DFT size (N_{DFT})
- Type of the window used
- Additional DSP techniques (Averaging, Zero padding, filters, etc.)

The frequency analysis is defined by the following equation:

$$f_{analysis}(m) = \frac{mfs}{N}$$

It is possible to see the DFT stage as a kind of band pass filter, whose central frequency is the frequency analysis, whose bandwidth and gain can be modified. The following figure shows the DFT model like a system input $x(n)$, which is a data sequence coming from the sampling stage, and the outputs as sequence of $X(m)$ being the calculation result of the DFT. We put in the figure the N_{DFT} , and window as the parameter used to adjust the bandwidth and gain

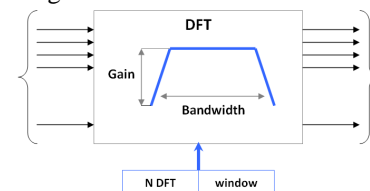


Figure 8. Bandpass DFT model at a given frequency component
The DFT result will produce results at all the frequency analysis indicating which amplitude exists in $x(n)$ at the frequency analysis calculated at a given point m . The figure 9 is a model for the whole DFT calculating.

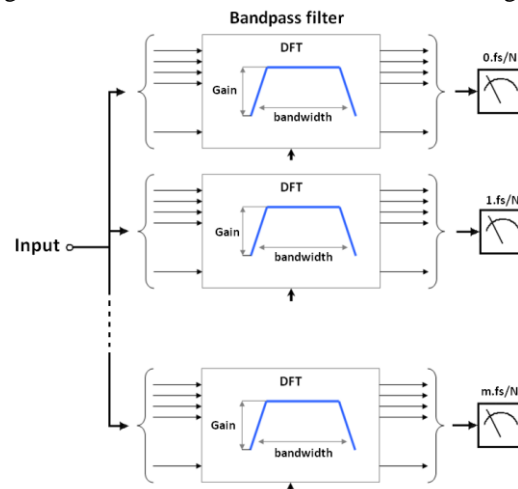


Figure 9. Bandpass DFT model

Every time we increase the N_{DFT} , we have a narrower bandwidth, which gives us the advantage of increasing the possibility of detection and separation energies; because as N_{DFT} is higher, the frequency resolution is better. Besides this advantage, the amount of the background noise is less present in the measurement. The figure 10 shows the example of this situation.

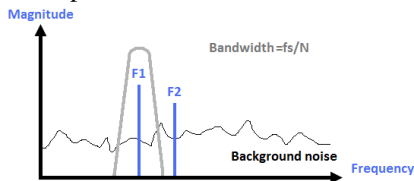


Figure 10. Narrow system measurement

Increasing the N_{DFT} has the inconvenient of increasing the processing time. Using less point N_{DFT} will reduce the resolution, and increase the bandwidth of the bandpass filter model. This situation is represented by the figure 11.

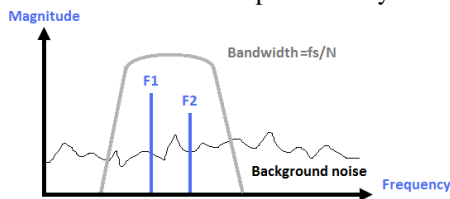


Figure 11. Wideband system measurement

In this situation we can't distinguish between signals F1 and signal F2, furthermore, the measurements will include more quantity of background noise

Let see an example to illustrate what we explained above. In the figure 12, we measure a 300Hz sinewave modulated en AM with 8 kHz, sampled at 48 kHz. We use a Hamming window.

In the case of figure 12a we take 256 N_{DFT} points and we represent the 128 first points, while the figure 12b, is a zoom representation. Notice that this measurement gives us information that we have at the input a signal of frequency 8.013 kHz.

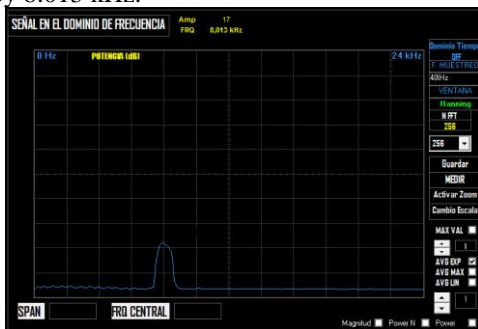


Figure 12a. 256 N_{DFT} point 300Hz sinewave modulated en AM with 8 kHz, sampled at 48 kHz

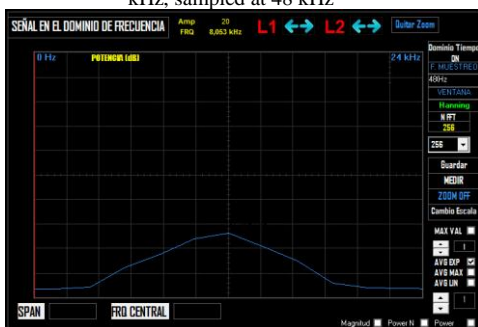


Figure 12b. 256 N_{DFT} point 300Hz sinewave modulated en AM with 8 kHz, sampled at 48 kHz

In figure 13a, we increase the number of points taken from 256 to 512. Then in figure 13b, we see that the main lobe form has changed, but it is difficult to decide if this situation is due to the apparition of noise or the presence of other frequency components near to the main lobe.

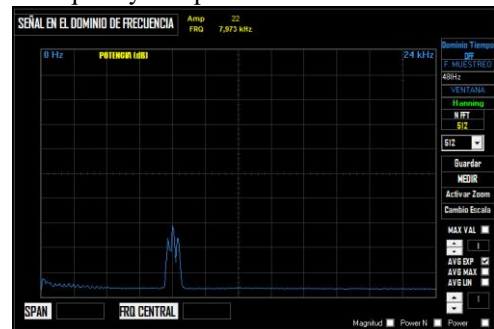


Figure 13a. 512 N_{DFT} point 300Hz sinewave modulated en AM with 8 kHz, sampled at 48 kHz

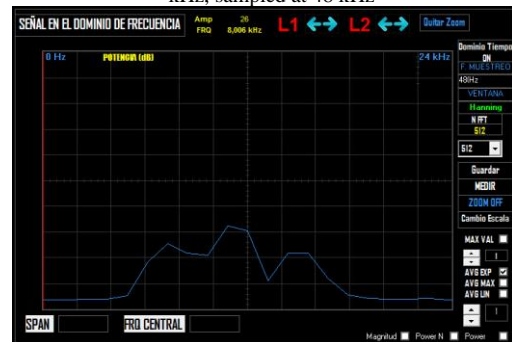


Figure 13b. 512 N_{DFT} point 300Hz sinewave modulated en AM with 8 kHz, sampled at 48 kHz

The figure 14 represents the case of taking 1024 DFT point. Now we can see that this signal contains more than one frequency component.

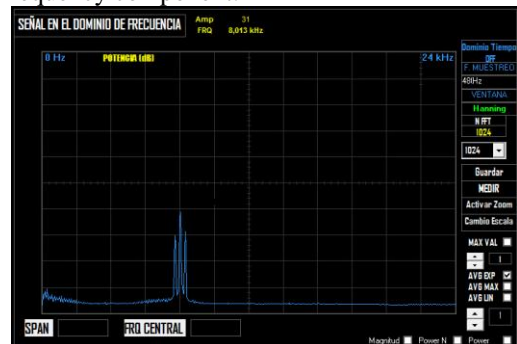


Figure 14a. 1024 N_{DFT} point 300Hz sinewave modulated en AM with 8 kHz, sampled at 48 kHz

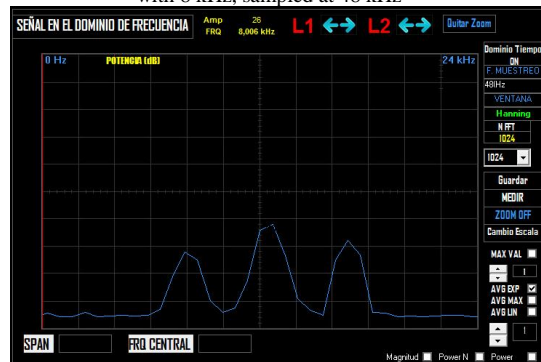


Figure 14b. 1024 N_{DFT} point 300Hz sinewave modulated en AM with 8 kHz, sampled at 48 kHz

Increasing the size of the DFT to 4096 points, we get the signal represented in the figure 15. We can now see with precision that we obtain a main lobe centered to the

frequency 8kHz with two sidebands, the right one with 8.3 kHz and the left one with 7.7 kHz

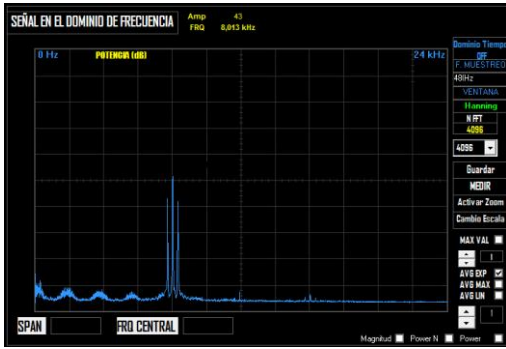


Figure 15a. 1024 N_DFT point 300Hz sine wave modulated en AM with 8 kHz, sampled at 48 kHz

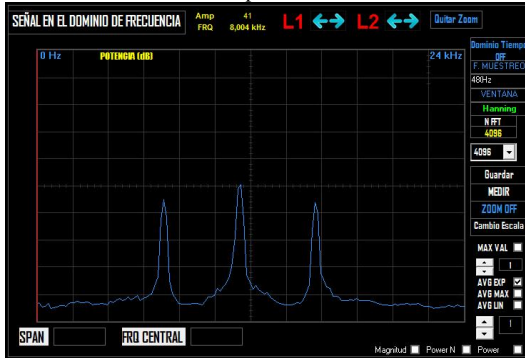


Figure 15b. 4096 N_DFT point 300Hz sine wave modulated en AM with 8 kHz, sampled at 48 kHz

Increasing the size of the DFT has the advantage of having more processing gain [2]. This involves the possibility of extracting signal that is tucked into noise. The output SNR of the DFT increases when the size N_DFT increases.

We demonstrate this by the following measurements made with our system measurement. The figure 16 is a 6 kHz sine-wave signal received through a wideband receiver. We plot the 128 outputs of a 256-point DFT. It is very difficult to detect the input signal of 6 kHz. If we change the size of DFT to 512 points, we can now see the presence of the input signal. Increasing the N_DFT to 1024 and 2048, we obtain the results shown in figure 16c, and 16d. As we can notice, the amplitude of the resulting frequency component increases as the number of points N_DFT increases. Also we see that the main lobe is narrower.

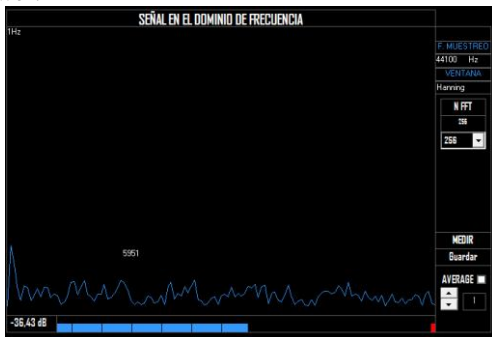


Figure 16a. 6 kHz sine-wave signal received through a wideband receiver

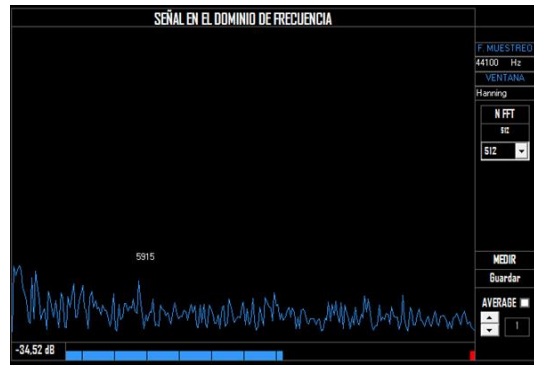


Figure 16b. 6 kHz sine-wave signal received through a wideband receiver

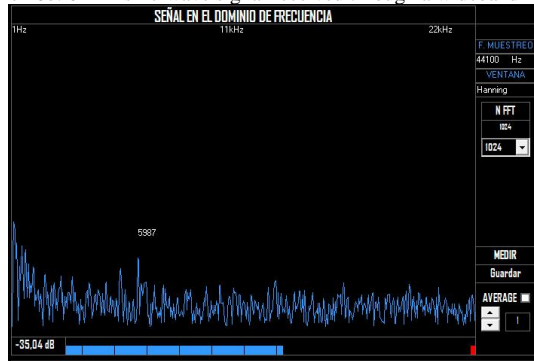


Figure 16c. 6 kHz sine-wave signal received through a wideband receiver

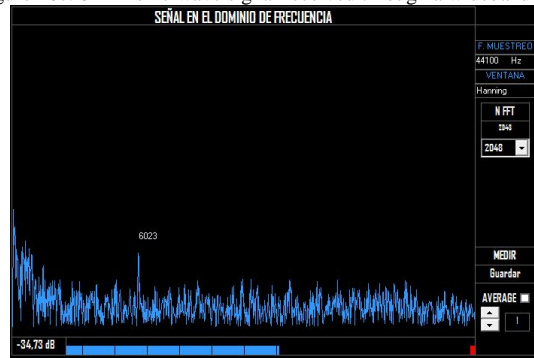


Figure 16d. 6 kHz sine-wave signal received through a wideband receiver

The signal-to-noise ratio (SNR) is defined [1,2] as the DFT’s output signal-power level over the average output noise-power level. The figure 16 shows also that the SNR increases when the DFT size increases.

The leakage has also the effect of increasing the effective background noise and reduces the DFT’s output SNR.

VII. Averaging

The averaging technique improves the accuracy and repeatability of measurements, especially with the presence of noise. When the level of the signal of interest is nearly equal to the noise level, it is difficult to extract this signal from noise. We implemented the averaging technique in order to overcome this trouble. The figure 17 shows the averaging techniques implemented into the system measurement presented in this paper.

Lineal Averaging

$$FFT_t(I) = (FFT(I) + FFT_{t-1}(I))/n$$

Exponential Averaging

$$FFT_t(I) = FFT(I) \cdot 1/N + FFT_{t-1}(I) \cdot (N-1)/N$$

Maximum Averaging

$$\text{If } FFT(I) > FFT_{t-1}(I) \text{ then } FFT_t(I) = FFT(I)$$

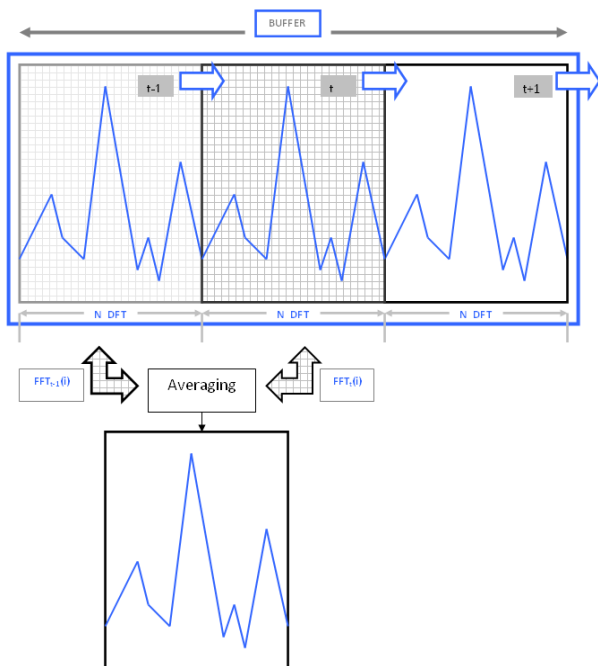


Figure 17. Averaging techniques implemented

We put an example of the results obtained when applying the averaging on a signal received with a wideband received with the presence of noise. This example measures a 13 kHz signal, modulated AM with 1MHz carrier. We take 1024 DFT points; we use a Hanning window, and a frequency sampling of 44.1 kHz.

The figure 18 shows the result obtained. We see in the figure 18a that is not possible to identify the signal received because we have a higher level of background noise.

When applying the average type “maximum”, we obtain the result shown in the figure 18b. Notice that the peak appears now clearly at 13 kHz.

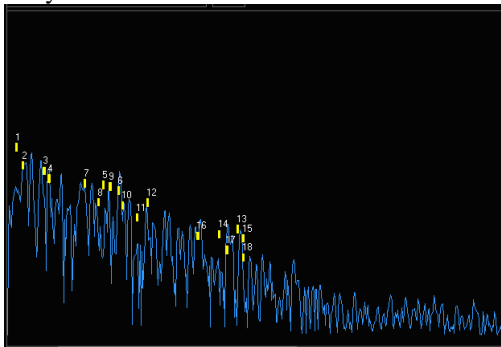


Figure 18a. Example measurement of a 13 kHz signal, modulated AM with 1MHz carrier

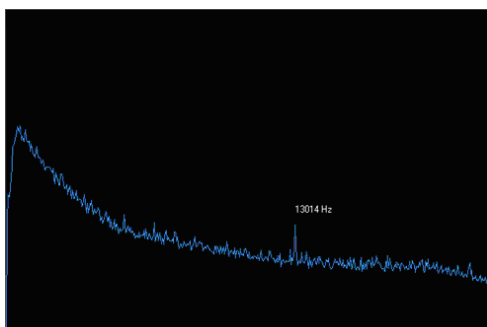


Figure 18b. Example measurement of a 13 kHz signal, modulated AM with 1MHz carrier

VIII. Conclusion

The demonstration measurement in this paper is made using the PC sound card as a tool of data acquisition. This solution presents the limitation of the sampling rate which is limited to 96 kHz, and the anti-aliasing filter which cut off signal up to 22 kHz.

We have presented the more relevant parameter to be manipulated in order to analyze and measure signals. Changing one parameter affects all the other parameter. Depending on the application, accordingly, we can decide to manipulate the adequate parameter.

We see that the size of the DFT is an important parameter which affects the improvement of the SNR, resolution, magnitude, but there are always tradeoffs between this improvement and the processing time that take the method to calculate the DFT.

References

- [1] A. Papoulis, “Signal Analysis” McGraw-Hill Book Company, New York, 1977, ISBN. 0-07-048460-0
- [2] Richard G. Lyons, Understanding Digital Signal Processing, Pearson Education, 2010, ISBN 0137028520, 9780137028528, 944 páginas
- [3] S.W. Smith; The Scientist and Engineer’s Guide to Digital Signal Processing, California Technical Publishing, 1997, ISBN 0966017633
- [4] Robinson, E.A., “A historical perspective of spectrum estimation,” Proceedings of the IEEE , Vol. 70, no. 9, pp. 885-907, Sept. 1982
- [5] J.W. Cooley and J.W. Tukey, “An algorithm for the machine calculation of complex Fourier Series,” Mathematics Computation, Vol. 19, 1965, pp 297-301
- [6] HV Sorensen and all, Real Valued Fast Fourier Transform Algorithms, IEEE Transactions on acoustics, speech, and signal processing, VOL. ASSP-35, NO. 6, June 1987
- [7] J. A GLASSMAN, “A generalization of the fast Fourier transform” IEEE Transactions on computers, VOL. C19, NO. 2, February 1970
- [8] GD Bergland, “A guided tour of the fast Fourier transforms,” IEEE Spectrum, vol. 6, pp. 41-52, July 1969
- [9] Aerospace & Defense Symposium 2012, Agilent Technologies, 31/05/2012, Madrid, Spain
- [10] Michael Cerna and Audrey F. Harvey, The Fundamentals of FFT-Based Signal Analysis and Measurement, National Instruments, application note 041, July 2000
- [11] Robert A. Witte, Electronic Test Instruments. Theory and Applications, Hewlett-Packard, New Jersey, 1993.
- [12] M. Bakkali, C. Mascareñas, & ALL, Feasibility Study of Advancing and Sitting up Power Line Communication (PLC) System under Circumstances of Electromagnetic Compatibility (EMC) on the Ships, 9th International Conference. Electrical Power Quality and Utilization, 9-11 de octubre de 2007, Barcelona, (Spain)

Mohammed Bakkali is a Telecommunications Engineer. He received a IEEA M.Sc from the Abdelmalek-Essaâdi University in Tangier, Morocco. He received the Diploma of Advanced Studies (DEA) in Maritime Radiocommunications from the Cadix University (Spain). Is currently doing the position “Control & Communication Engineer” with CIAT and doing his research (PhD) under the guidance of Prof. Dr Carlos Mascareñas y Perez Iñigo, Cadix University.



Carlos Mascareñas y Perez Iñigo is Assistant Professor at the Radioelectronic Engineering School of the Cadix University (Spain). He is 1st Class ITU Radioelectronic Officer Certificated and also he is the leader of the Research groupe “Signals, Systems and Naval Communications” (<http://marconi.uca.es>). His scientific interests include Radiocommunications, Radiopropagation, Electromagnetic Compatibility, Maritime Safety and Protection.

